0022-3565/08/3242-507–516$20.00
THE JOURNAL OF PHARMACOLOGY AND EXPERIMENTAL THERAPEUTICS
JPET 324:507–516, 2008

Vol. 324, No. 2
126938/3300851
Printed in U.S.A.

Gene Expression Analysis in Rats Treated with Experimental Acetyl-Coenzyme A Carboxylase Inhibitors Suggests Interactions with the Peroxisome Proliferator-Activated Receptor α Pathway

Jeffrey F. Waring, Yi Yang, Christine H. Healan-Greenberg, Andrew L. Adler, Robert Dickinson, Teresa McNally, Xiaojun Wang, Moshe Weitzberg, Xiangdong Xu, Andrew Lisowski, Scott E. Warder, Yu Gui Gu, Bradley A. Zinker, Eric A. Blomme, and Heidi S. Camp

Abbott Laboratories, Abbott Park, Illinois

Received June 8, 2007; accepted November 15, 2007

ABSTRACT

Acetyl CoA carboxylase (ACC) 2, which catalyzes the carboxylation of acetyl-CoA to form malonyl-CoA, has been identified as a potential target for type 2 diabetes and obesity. Small-molecule inhibitors of ACC2 would be expected to reduce de novo lipid synthesis and increase lipid oxidation. Treatment of *ob*/*ob* mice with compound A-908292 (S) ({(*S*)-3-[2-(4-isopropoxy-phenoxy)-thiazol-5-yl]-1-methyl-prop-2-ynyl}-carbamic acid methyl ester), a small-molecule inhibitor with an IC_{50} of 23 nM against ACC2, resulted in a reduction of serum glucose and triglyceride levels. However, compound A-875400 (R) ({(*R*)-3-[2-(4-isopropoxy-phenoxy)-thiazol-5-yl]-1-methyl-prop-2-ynyl}-carbamic acid methyl ester), an inactive enantiomer of A-908292 (S) with approximately 50-fold less activity against ACC2, also caused a similar reduction in glucose and triglycerides, suggesting that the glucose-lowering effects in *ob*/*ob* mice may be mediated by other metabolic pathways independent of ACC2 inhibition. To characterize the pharmacological activity of these experimental compounds at a transcriptional level, rats were orally dosed for 3 days with either A-908292 (S) or A-875400 (R), and gene expression analysis was performed. Gene expression analysis of livers showed that treatment with A-908292 (S) or A-875400 (R) resulted in gene expression profiles highly similar to known peroxisome proliferator-activated receptor (PPAR)-α activators. The results suggest that, in vivo, both A-908292 (S) and A-875400 (R) stimulated the PPAR-α-dependent signaling pathway. These results were further supported by both an in vitro genomic evaluation using rat hepatocytes and immunohistochemical evaluation using 70-kDa peroxisomal membrane protein. Overall, the gene expression analysis suggests a plausible mechanism for the similar pharmacological findings with active and inactive enantiomers of an ACC2 inhibitor.

The incidence of type 2 diabetes has dramatically increased over the past decade. This epidemic is largely attributed to the proliferation of key risk factors, which include a sedentary lifestyle, a high-fat diet, obesity, and the demographic shift to a more aged population. There is ample evidence that abdominal obesity and physical inactivity contribute significantly to the development of type 2 diabetes (Turkoglu et al., 2003; Steyn et al., 2004). At the cellular level, an increase in ectopic fat storage in nonadipose tissues such as skeletal muscle, liver, and pancreas is a strong predictor of the development of insulin resistance and type 2 diabetes (Sinha et al., 2002; Hulver et al., 2003). In addition, deregulation of fatty acid metabolism also contributes to the overall development of metabolic syndrome. Thus, targeting key enzymes that are critically involved in lipid synthesis, lipid oxidation, and/or triglyceride synthesis pathways with

J.F.W. and Y.Y. contributed equally to this work.

Article, publication date, and citation information can be found at http://jpet.aspetjournals.org.
doi:10.1124/jpet.107.126938.

ABBREVIATIONS: ACC, acetyl CoA carboxylase; A-908292, {(*S*)-3-[2-(4-isopropoxy-phenoxy)-thiazol-5-yl]-1-methyl-prop-2-ynyl}-carbamic acid methyl ester; A-875400, {(*R*)-3-[2-(4-isopropoxy-phenoxy)-thiazol-5-yl]-1-methyl-prop-2-ynyl}-carbamic acid methyl ester; PPAR, peroxisome proliferator-activated receptor; LC, liquid chromatography; MS, mass spectrometry; ANOVA, analysis of variance; IVT, In Vitro Technologies; HMGCS2, 3-hydroxy-3-methylglutaryl-CoA synthase; PMP70, 70-kDa peroxisomal membrane protein; A-859610, {3-[2-(4-isopropoxy-phenoxy)-thiazol-5-yl]-1-methyl-prop-2-ynyl}-carbamic acid methyl ester; GW7647, 2-(4-(2-(1-cyclohexanebutyl)-3-cyclohexylureido)ethyl)phenylthio)-2-methylpropionic acid.

small-molecule inhibitors would probably cause a reduction of fat accumulation in nonadipose tissues, notably in liver and skeletal muscles, and would therefore improve insulin sensitivity and overall lipid profiles.

Acetyl CoA carboxylase (ACC) catalyzes the carboxylation of acetyl-CoA to form malonyl-CoA. Malonyl-CoA, in turn, can be used by fatty acid synthase for de novo lipogenesis and also acts as a potent allosteric inhibitor of carnitine palmitoyltransferase 1, a mitochondrial membrane protein that shuttles long-chain fatty acyl CoAs into the mitochondria where they are oxidized (Ruderman and Prentki, 2004). In rodents and in humans, there are two isoforms of ACC encoded by distinct genes, but sharing overall 70% amino acid identity. ACC1, a 265-kDa cytosolic protein, is highly expressed in lipogenic tissues, such as liver and adipose tissue, whereas the 280-kDa ACC2 protein is preferentially expressed in oxidative tissues like skeletal muscle, heart, and, to some extent, liver (Abu-Elheiga et al., 1997; Mao et al., 2003). ACC2 has a unique N terminus domain comprised of 114 amino acids that represent a putative transmembrane domain thought to be responsible for mitochondrial targeting (Abu-Elheiga et al., 2000). It has been shown that whole-body knockout of ACC2 in mice shows a favorable metabolic profile; the mice are resistant to high-fat diet-induced obesity and show decreased lipid content in both liver and adipose (Oh et al., 2005). The liver lipid content in the ACC2$^{-/-}$ mouse was described in Abu-Elheiga et al. (2001).

Small-molecule inhibitors of ACC2 have been synthesized at Abbott Laboratories (Abbott Park, IL). These compounds have been shown to lower malonyl-CoA in skeletal muscle and to a lesser extent in liver in Sprague-Dawley rats (Gu et al., 2006; Xu et al., 2007). A-859610 is a racemic mixture of A-908292, the active (S) enantiomer (IC_{50} = 0.023 μM for human ACC2 and >30 μM for human ACC1) and A-875400, the less active (R) enantiomer (IC_{50} = 1.082 μM for human ACC2 and >30 μM for human ACC1). In a previous study, in *ob*/*ob* mice, the racemate, A-859610, dosed at 30 mg/kg/day (b.i.d., p.o.) for 2 weeks was shown to lower serum glucose by approximately 30% (data not shown). We were surprised to find that in a 2-week repeat-dose study, both the active and inactive enantiomers of A-859610 showed a reduction in glucose and triglycerides to a similar extent, indicating a potential off-target effect.

To better characterize the active and inactive enantiomers of A-859610, microarray analysis was performed on rats treated with either A-908292 (S) or A-875400 (R). The results suggest that both compounds behave as activators of the peroxisome proliferator-activated receptor (PPAR)-α pathway in vivo, which is most probably the underlying mechanistic basis for glucose and triglyceride lowering in *ob*/*ob* mice. These results are an example of how gene expression profiling can aid in determining the mechanistic action of certain pharmacological agents.

Materials and Methods

Animals and Treatment. *ob*/*ob* mice (6–7 weeks of age; The Jackson Laboratory, Bar Harbor, ME) were acclimated to the animal research facilities for 5 days. The *ob*/*ob* mice were obtained and treated as in previous publications (Zinker et al., 2002; Waring et al., 2003). Mice were fed a standard diet of Lab Diet Rodent Laboratory Diet 5105. The *ob*/*ob* mice were dosed with vehicle (n = 10), A-875400 (R) (n = 9), or A-908292 (S) (n = 9) at 30 mg/kg/day (b.i.d., p.o.) for 2 weeks. For the malonyl-CoA rat study, normal Sprague-Dawley rats (n = 6) were fasted for 4 h and then orally dosed with 10 and 50 mg/kg of either A-908292 (S) or A-875400 (R), followed by oral gavage of high-carbohydrate-enriched meals.

For the gene expression analysis study, Sprague-Dawley rats [Crl:CD(SD)IGS BR] weighing between 201 and 221 g were obtained from Charles River Laboratories, Inc. (Portage, MI). Rats were fed a standard diet of Lab Diet Rodent Laboratory Diet 5001 pellets (PMI Nutrition International, Inc., St. Louis, MO). Rats were dosed with vehicle (sterile H_2O containing 1% Tween) (n = 3), A-875400 (R) (n = 3) or A-908292 (S) (n = 3) at 30 or 100 mg/kg/day b.i.d. for a period of 3 days. The dose volume for all treatment groups was 4 ml/kg/dose. All rats were fasted overnight after their last treatment and euthanized under CO_2 anesthesia. In a separate study, Sprague-Dawley rats [Crl:CD(SD)IGS BR] weighing between 201–221 g were obtained from Charles River Laboratories, Inc. Rats were fed a standard diet of Lab Diet Rodent Laboratory Diet 5001 pellets (PMI Nutrition International, Inc.). Rats were dosed with vehicle (sterile H_2O containing 1% Tween) (n = 3) or bezafibrate at 200 mg/kg/day b.i.d. for a period of 3 days. The dose volume for all treatment groups was 4 ml/kg/dose. All rats were fasted overnight after their last treatment and euthanized under CO_2 anesthesia.

All tissues collected for gene expression analysis were immediately flash frozen in liquid nitrogen and subsequently stored at −70°C. For histopathology evaluation, livers from rats were fixed in 10% neutral buffered formalin. Blood samples drawn from the animals at necropsy were used to measure serum concentrations or activities of blood urea nitrogen, creatinine, alanine amino transferase, aspartate amino transferase, gamma glutamyltransferase, alkaline phosphatase, cholesterol, triglycerides, bilirubin, glucose, total protein, albumin, and globulins using an Abbott Aeroset clinical chemistry analyzer.

For the immunohistochemistry and electron microscopy study, rats were dosed once daily for 5 days with A-875400 (R) (100 mg/kg/day), bezafibrate (200 mg/kg/day), or vehicle [sterile H_2O containing 1% Tween for A-875400 (R), 0.2% hydroxypropyl methylcellulose for bezafibrate]. Immunohistochemistry samples from rats treated with A-908292 (S) were obtained from the 3-day study used for gene expression analysis. Experiments were conducted in accordance with the Guiding Principles in the Use of Animals in Toxicology (Society of Toxicology, 2002) and approved by the local Institutional Animal Care and Use Committee.

Malonyl-CoA and ACC2 Activity. Sprague-Dawley rats or *ob*/*ob* mice were sacrificed; subsequently, liver and soleus muscle were immediately removed and snap frozen in liquid nitrogen. The tissues were homogenized with a Polytron in the extraction solution (ice-cold 5% 5-sulfosalicylic acid containing 50 μM 1,4-dithioerythreitol) with the ratio 1:10 (w/v). The tissue homogenates were centrifuged at 14,000*g* for 15 min at 4°C. The clear supernatants were then filtered through 0.22-μm pore size filtering discs before being injected into the LC/MS system for the detection of the short-chain acyl-CoAs. Assays for determination of human ACC1 and ACC2 activity and LC/MS results for malonyl-CoA were as described previously (Gao et al., 2007).

Gene Expression Analysis. Livers were collected from all rats and flash frozen in liquid nitrogen and subsequently stored at −70°C. Frozen liver samples (approximately 100 mg of tissue per sample) were immediately added to 2 ml of TRIzol reagent (Invitrogen, Carlsbad, CA) and homogenized using a Polytron 300D homogenizer (Brinkman Instruments, Westbury, NY). One milliliter of the tissue homogenate was transferred to a microfuge tube, and total RNA was extracted via chloroform extraction followed by nucleic acid precipitation with isopropanol. The pellet was washed with 75% ethanol and resuspended in molecular biology grade water. Nucleic acid concentration was determined by o.d. 260 nm (Smart-Spec; Bio-Rad Laboratories, Hercules, CA), and RNA integrity was evalu-

ated using an Agilent bioanalyzer (model 2100; Agilent Technologies, Foster City, CA).

Microarray analysis was performed using the standard protocol provided by Affymetrix Inc. (Santa Clara, CA) and as described previously (Waring et al., 2001b). The microarray scanned image and intensity files (.cel files) were imported into Rosetta Resolver gene expression analysis software, version 5.0 (Rosetta Inpharmatics, Seattle, WA). Samples from all individual rats were hybridized to the Affymetrix RAE230A chip. Individual expression profiles from treated rats were compared with an in silico pool of expression profiles from the vehicle-treated rats. Genes were considered significantly regulated if the *p* value assigned to the gene by Resolver was less than or equal to 0.01. Data analysis was also conducted using DrugMatrix version 3.10 (Iconix Pharmaceuticals, Mountain View, CA) (Ganter et al., 2005). The similarity of gene expression profiles of the test compound and reference compounds from the DrugMatrix database was calculated as the Pearson's correlation coefficient based on the common genes shared by the Affymetrix RAE230A and Codelink RU1 (GE Healthcare, Piscataway, NJ). The affect on pathways was calculated as the percentage of perturbation with a *p* value determined by hypergeometric distribution.

To detect significant gene expression changes induced by the A-908292 (S) and A-875400 (R), the gene expression ratios from rats treated at 100 mg/kg/day were analyzed by error-weighted one-way ANOVA with Benjamini and Hochberg multiple testing correction using the Rosetta Resolver system. Probes with a false discovery rate less than or equal to 0.01 were considered statistically significant.

In Vitro Studies. Primary rat hepatocytes were obtained as described previously (Waring et al., 2001a). Rat hepatocytes were plated at a density of 800,000 cells/ml with 10 ml of InVitroGro Hepatocyte Medium (In Vitro Technologies, Baltimore, MD), on 100-mm BD BioCoat Collagen I Cellware (Becton Dickinson, Bedford, MA), at 37°C and 5% CO_2. Rat hepatocytes were treated for 24 h with A-908292 (S) and A-875400 (R) at a concentration of 100 μM, which is the maximum feasible dose due to limited solubility. The cells were treated with each compound in duplicate. Cells were harvested for RNA using TRIzol reagent, and microarray analysis was performed as described above.

The in vitro signature for PPAR-α agonism, which consists of 11 genes, was configured by identifying genes consistently regulated by known peroxisome proliferators in isolated rat hepatocytes. The signature was created using linear discriminant analysis, as described previously (Yang et al., 2006).

Cryopreserved plateable human hepatocytes were obtained from In Vitro Technologies (IVT; catalog number M/F00995-P). Hepatocytes were thawed in a 37°C water bath, than decanted into InVitroGro CP Medium (IVT catalog number Z990003). Cell count and viability was determined by Trypan blue exclusion, and cells were diluted in CP medium to a concentration of 0.7 × 106 viable cells/ml. Cells were plated on 12- or 24-well collagen-coated plates, then placed in a 37°C, 5% CO_2 incubator. After overnight incubation, CP medium was aspirated off, cells were washed with phosphate-buffered saline, and InVitroGro HI Medium (IVT catalog number Z990012) was added to the wells. Cells were incubated overnight in HI medium and then treated for 24 h with the compounds of interest. After RNA isolation, samples were assayed using the TaqMan EZ RT-PCR kit (Applied Biosystems, Foster City, CA; part number N808-0236). The probes for CYP4A11 are as follows: GGC GTC TCT GTG TAC AAA AGG AA, forward; TGA AGA AGC AGA GGG AGC AAA, reverse; and /56-FAM/TGG CAT TCA GAG CAC CCC ATG GA/3BHQ_1/, TaqMan. The probe sequences for 3-hydroxy-3-methylglutaryl-CoA synthase (HMGCS2) are as follows: GCC TTT TCC CAG GTA CTT GGT, forward; CGC CGG GCA TAC TTT CG, reverse; and /56-FAM/TGC TGC TCG TCC ACT CGC TCC AG/3BHQ_1/, TaqMan.

The PPAR-α reporter assay is comprised of three constructs: 1) a reporter gene, pG5E1bluc, which comprises five gal4 DNA binding sites fused upstream of the luciferase gene in the vector pGL2 basic (Promega, Madison, WI) (Hsu et al., 1994); 2) a chimeric PPAR-α construct, pSV40/gal4 DBDneo. In this construct, the DNA binding domain of Gal4 is fused to the ligand-binding domain (amino acids 167–468); and 3) the plasmid pCMVbgal as a normalization control to ensure even transfection and cell growth throughout the plate (Lehmann et al., 1995). Plasmids were transfected by electroporation into HepG2 cells at the following ratio: 9 μg of chimeric PPAR, 9 μg of reporter, and 1 μg of pCMVbgal. The final concentration of plasmids used was optimized by varying the ratio of chimeric construct to reporter construct to determine the optimum window. Approximately 24 h after electroporation, cells were treated with a known PPAR-α reference compound GW7647 or with A-875400 (R) or A-908292 (S) at concentrations ranging from 0.003 to 30 μM. After compound incubation for 48 h, cells were washed with PBS, and luciferase activity was performed using the Promega luciferase assay (Promega; catalog number E1500).

Histopathology and Immunohistochemistry Staining for 70-kDa Peroxisomal Membrane Protein. For histopathology evaluation, livers from rats were fixed in 10% neutral buffered formalin, routinely processed, and embedded in paraffin. Paraffin sections (5 μm) stained with hematoxylin were evaluated.

Histologic slides (5 μm) were also used to evaluate 70-kDa peroxisomal membrane protein (PMP70) expression by immunohistochemistry (Colton et al., 2004). In brief, paraffin sections (5-μm-thick) were progressively rehydrated with a series of xylene and alcohol. Antigen retrieval with citrate buffer was performed using a rice cooker for 20 min. Immunohistochemistry staining was performed using the avidin-biotin complex technique for detection of antibodies to PMP70. Sections were incubated with the primary antibody PMP70 (PAI-650; Affinity Bioreagents, Golden, CO) at room temperature for 1 h at a dilution of 1:500. Biotinylated secondary antibody (goat anti-rabbit; Vector Laboratories, Burlingame, CA) was applied at room temperature for 30 min at a concentration of 1:200. Sections were incubated with DAB Chromagen (Sigma-Aldrich, St. Louis, MO) for 1 min, which gave the optimal color development. Sections were then counterstained with hematoxylin for 2 min and then coverslipped and evaluated.

Electron Microscopy. Specimens of liver collected for ultrastructural pathology were fixed by immersion in Karnovsky's fixative, pH 7.3. Specimens were postfixed in 1% osmium tetroxide in 0.1 M Sorensen's phosphate buffer, pH 7.3, dehydrated in graded ethanol and propylene oxide, and embedded in Luft's epoxy resin. Ultrathin sections were cut, stained with 2% methanolic uranyl acetate followed by Reynolds' lead citrate, and examined using a LEO 910 transmission electron microscope.

Western Blotting. Rat liver sections were suspended in a 1:1 mixture of T-PER (Pierce, Rockford, IL) and a lysis buffer, pH 7.5, consisting of HEPES (50 mM), Triton 100 (0.5%), NaCl (150 mM), EDTA (1 mM), and EGTA (1 mM), and supplemented with protease inhibitors (Roche, Indianapolis, IN). The tissue was homogenized and rocked at 4°C for 20 min followed by centrifugation (20,000*g*). The supernatants were removed, and protein-normalized aliquots were separated on a Novex 4–12% Bis-Tris SDS-polyacrylamide gel electrophoresis according to the manufacturer's protocol (Invitrogen). The protein was transferred to polyvinylidene difluoride, followed by blocking with Odyssey blocking buffer (LI-COR Biosciences, Lincoln, NE). The blot was probed with a rabbit polyclonal PMP70 antibody (Novus Biologicals Littleton, CO), followed by addition of an anti-rabbit secondary antibody labeled with an IR dye. The blot was imaged and the bands quantified on the Odyssey Infrared Imaging System (LI-COR Biosciences).

Results

Alkynyl Subseries of ACC2 Inhibitors. Chemical structures for A-908292 (S) and A-875400 (R) are shown in Fig. 1A, along with their respective IC_{50}s against hACC1 and

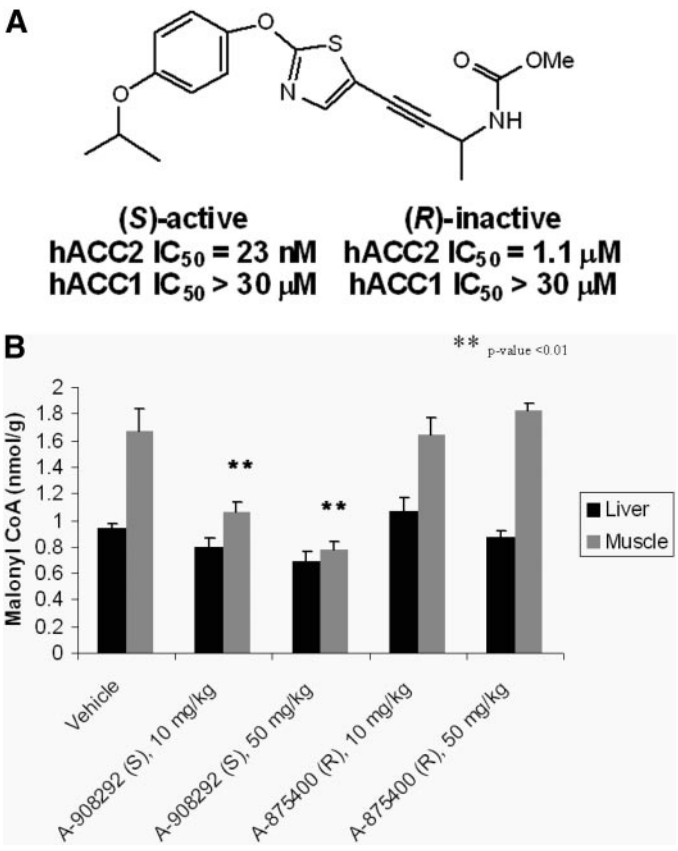

Fig. 1. A, chemical structure of A-859610, the racemate of A-908292 (S) and A-875400 (R). B, levels of malonyl-CoA in Sprague-Dawley rats in liver (black bars) and muscle (gray bars) after treatment with A-908292 (S) and A-875400 (R). The malonyl-CoA levels represent an average from six rats in each treatment group. The asterisks represent a significant change ($p < 0.01$) from vehicle-treated controls, as measured using ANOVA with post hoc Dunnett's.

hACC2. The (S) enantiomer A-908292 (S) is highly selective for hACC2 versus hACC1 (IC_{50} = 0.023 μM for hACC2 and >30 μM for hACC1), whereas the (R) enantiomer A-875400 (R) is less active against hACC2 with an approximate IC_{50} of 1.08 μM. Both compounds are relatively weak inhibitors of hACC1 (IC_{50} > 30 μM). Rat pharmacokinetics was performed on the racemate A-859610. The compound displayed 80% bioavailability, with low clearance and a relatively long half-life (data not shown). Because ACC catalyzes the formation of mCoA, it is expected that the inhibition of ACC via small-molecule inhibitors should decrease mCoA production, such that an acute in vivo screening model was developed to demonstrate on-target activity of ACC inhibitors. In brief, 4-h fasted Sprague-Dawley rats were orally dosed with 10 and 50 mg/kg of either A-908292 (S) or A-875400 (R), followed by oral gavage of high-carbohydrate-enriched meals; as a result, liver and muscle tissues were excised and subjected to LC/MS-based quantitation of mCoA levels (Gao et al., 2007). A-908292 (S) caused a dose-dependent reduction of malonyl-CoA in the muscle at both 10 and 50 mg/kg relative to vehicle-treated control. In addition, a small but significant reduction in malonyl-CoA levels was seen in the liver after the 50 mg/kg treatment with A-908292 (S). The greater reduction in malonyl-CoA levels seen in muscle compared with liver probably reflects that ACC2 is predominantly expressed at high levels in muscle and at much lower levels in liver (Abu-Elheiga et al., 1997). In contrast, compound A-875400 (R) did not result in a reduction in malonyl-CoA levels in either muscle or liver in either dose group (Fig. 1B). The results firmly demonstrate on-target mechanisms of A-908292 (S) in vivo.

Chronic Study in *ob/ob* Mice. *ob/ob* Mice were treated with 30 mg/kg A-908292 (S) or A-875400 (R) for 2 weeks. Plasma glucose levels were determined on days 1, 7, and 15, and plasma triglyceride levels were measured at the end of the study on day 15. Treatment with both A-908292 (S) and A-875400 (R) resulted in a significant decrease of plasma glucose and triglyceride levels on day 15 (Fig. 2, A and B). Despite the differential activity against ACC2, both compounds decreased glucose and triglycerides to a similar degree. Malonyl-CoA levels in muscle and liver were measured in the *ob/ob* mice after 2-week drug treatment. As expected, A-908292 (S) treatment resulted in a reduction of malonyl-CoA levels relative to vehicle-treated control. In contrast, as seen previously in the acute study, no reduction of mCoA was observed with A-875400 (R) (Fig. 3). Similar to what was observed in Sprague-Dawley rats, treatment with both A-908292 (S) and A-875400 (R) did not result in a decrease in malonyl-CoA levels in liver. In fact, both compounds seemed to cause a small increase in liver malonyl-CoA levels (Fig. 3). The significance of the increase in malonyl-CoA levels is not known.

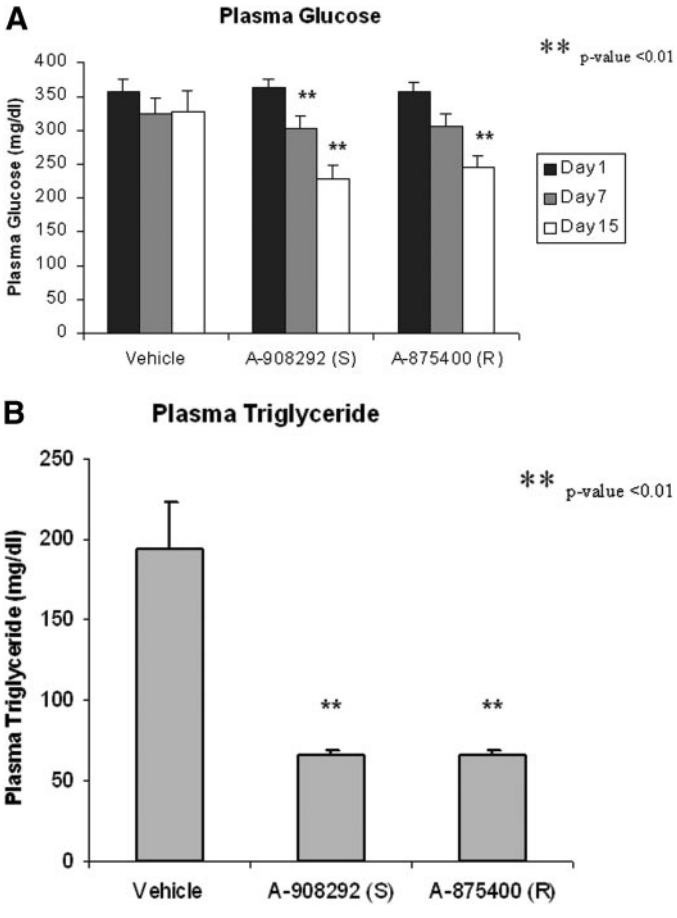

Fig. 2. Plasma glucose (A) and triglyceride levels (B) in *ob/ob* mice treated at 30 mg/kg/day (b.i.d., p.o.) for 2 weeks with vehicle (n = 10), A-908292 (S) (n = 9), and A-875400 (R) (n = 9). The asterisks represent a significant change ($p < 0.01$) from vehicle-treated controls, as measured using ANOVA with post hoc Dunnett's.

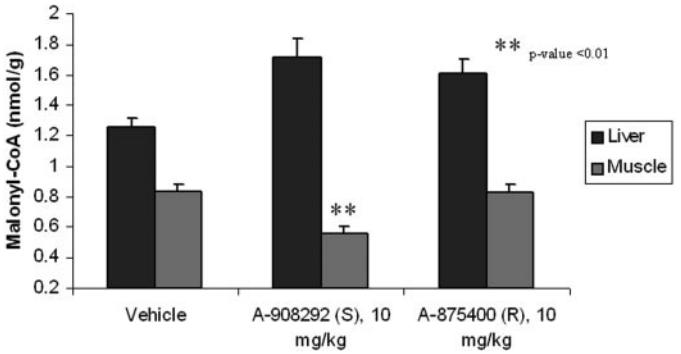

Fig. 3. Malonyl CoA determination in muscle and liver in *ob/ob* mice after treatment with A-908292 (S) and A-875400 (R). The treatment conditions are the same as in Fig. 2. The asterisks represent a significant decrease ($p < 0.01$) from vehicle-treated controls, as measured using ANOVA with post hoc Dunnett's.

Gene Expression Study in Sprague-Dawley Rats. To further characterize, the pharmacological activity of A-908292 (S) and A-875400 (R), male Sprague-Dawley rats were treated with the compounds at doses of 30 and 100 mg/kg for 3 days, and gene expression profiles from various tissues were analyzed. Sprague-Dawley rats were used to compare the gene expression signatures from A-908292 (S) and A-875400 (R) to the DrugMatrix database, which contains expression profiles from over 1000 compounds treated in rats. No significant serum chemistry changes were observed in the rats treated with the inactive enantiomer, A-875400 (R) at either dose. The active enantiomer, A-908292 (S), caused mild, dose-related serum cholesterol increases (Table 1). In the liver of two of three rats treated with A-875400 (R) at the high dose, random hepatocellular apoptosis was observed. Histopathological examination of the liver from A-908292 (S)-treated rats at the high dose showed random hepatocellular apoptosis, hepatocellular hypertrophy, and an increase in mitotic activity of hepatocytes.

Gene expression analysis was conducted on livers from the rats in all treatment groups. Compound-induced gene expression changes were identified relative to the vehicle-treated controls. Similar patterns of gene expression changes were seen in the livers of rats treated with A-908292 (S) or A-875400 (R) at the low and high doses (Fig. 4). For the high-dose treatment groups, treatment with A-908292 (S) or A-875400 (R) resulted in a significant regulation of 214 and 130 genes, respectively. Of these, 100 genes were regulated in common. The higher number of gene expression changes induced by A-908292 (S) may reflect the higher levels of the compound in liver, relative to A-875400 (R) (Fig. 4). A thorough analysis of the gene expression changes was performed. In particular, the expression profiles induced in the liver by treatment with the ACC compounds were compared with the liver expression profiles present in the Iconix DrugMatrix database. The liver expression profiles from rats treated with both A-908292 (S) and A-875400 (R) correlated with several experiments within DrugMatrix (Table 2). The majority of these reference compounds are known PPAR-α agonists, including bezafibrate, clofibrate, fenofibrate, and nafenopin. Pathway analysis within DrugMatrix was performed on the liver expression profiles from rats treated with A-908292 (S), A-875400 (R), and bezafibrate as a reference compound. The pathways that were the most significantly regulated by the three compounds are shown in Table 3. These pathways were affected to a similar extent by all three compounds and include PPAR-α and fatty acid metabolism, fatty acid biosynthesis, and β-oxidation. Figure 5 shows a comparison between the PPAR-α agonist bezafibrate relative to A-908292 (S) and A-875400 (R) for the genes in the PPAR-α pathway.

Both A-908292 (S) and A-875400 (R) were tested in isolated rat hepatocytes and analyzed using a gene expression signature for PPAR-α agonism (Yang et al., 2006). The assay was performed as described under *Materials and Methods*. The signature consists of 11 genes. Compounds are classified as being positive or negative for PPAR-α agonism based on their regulation of these 11 genes (Yang et al., 2006). The results showed that both compounds tested positive for the PPAR-α signature. In addition, several genes that are known to be regulated by PPAR-α, including acyl-CoA oxidase, acyl-CoA dehydrogenase, and acyl-CoA synthetase, were up-regulated by treatment with A-908292 (S) and A-875400 (R) in the isolated rat hepatocytes. The log(10) ratio value for the 11 genes in the PPAR-α signature, as well as for acyl-CoA oxidase, acyl-CoA dehydrogenase, and acyl-CoA synthetase, are shown in Table 4.

Immunohistochemical Staining. To further verify the PPAR-α effect suggested by the gene expression analysis, immunohistochemistry staining was performed for evidence of peroxisome proliferation. Rats were treated with vehicle, A-908292 (S), A-875400 (R) (100 mg/kg/day), or bezafibrate (200 mg/kg/day), which served as a positive control. Immunohistochemistry was performed using an antibody against the PMP70, which has been shown to be a hallmark of peroxisome proliferation (Colton et al., 2004). Figure 6A shows that treatment with bezafibrate, A-908292 (S), and A-875400 (R) resulted in an increase in PMP70 staining relative to vehicle-treated controls, indicating that treatment with both compounds induced peroxisome proliferation.

To quantify the immunohistochemistry results for PMP70, a Western blot was performed on extracts from livers treated with A-908292 (S) and A-875400 (R). Figure 6B shows that treatment with both compounds resulted in a 2- to 4-fold increase in PMP70 protein levels.

Finally, to definitively identify whether the ACC2 inhibitors were inducing peroxisome proliferation, electron microscopy was performed on livers from rats treated with

TABLE 1
Average clinical chemistry values from rats (n = 3/treatment group) treated with A-875400 (R) or A-908292 (S)

Compound	Dose	Alanine Amino Transferase	Aspartate Amino Transferase	Alkaline Phosphatase	Cholesterol	Trigylcerides	Glu
	mg/kg						
Vehicle	0.0	38.7	115.0	282.3	69.3	40.7	125.3
A-875400 (R)	30.0	37.3	110.7	328.0	60.0	32.3	96.7
A-875400 (R)	100.0	46.0	89.7	232.7	77.3	49.7	78.3
A-908292 (S)	30.0	40.7	108.0	290.7	88.0	39.0	77.3
A-908292 (S)	100.0	52.0	110.3	308.3	114.0	50.7	75.0

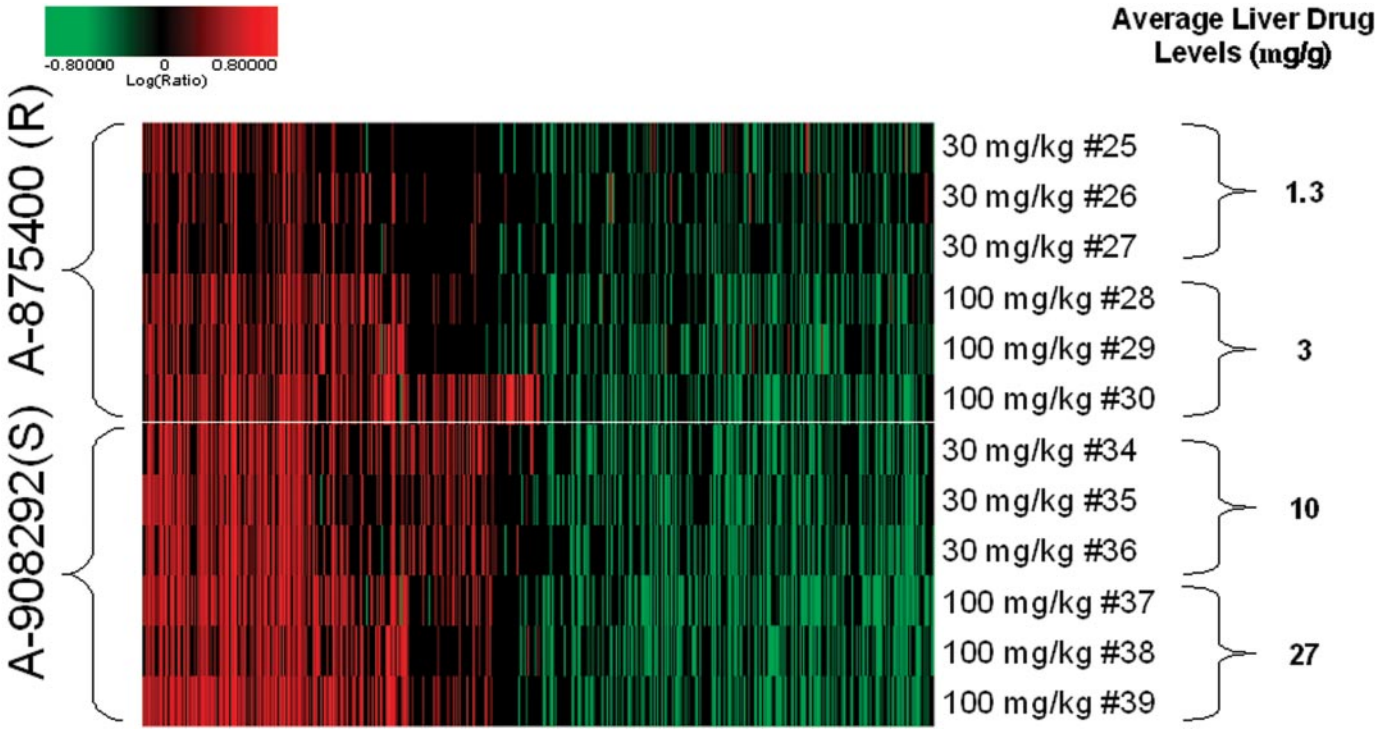

Fig. 4. Heat map showing gene expression changes in liver from Sprague-Dawley rats treated at 30 or 100 mg/kg for 3 days with A-908292 (S) and A-875400 (R). There were three rats per treatment group. Genes shown in red are up-regulated, whereas genes shown in green are down-regulated relative to vehicle-treated controls. Average liver drug levels (milligrams per gram) are shown for each animal. Genes shown were regulated 2-fold or greater in at least two rats, with a p value of 0.01 or lower.

TABLE 2
DrugMatrix Reference Compounds that induced gene expression changes in rat liver similar to those induced by A-908292 (S) and A-875400 (R)

Compound	Therapeutic Class	Compound Activity
Bezafibrate	Hypolipidemic agent	PPAR-α agonist
Fenofibrate	Hypolipidemic agent	PPAR-α agonist
Pirinixic Acid	Hypolipidemic agent	PPAR-α agonist
Clofibrate	Hypolipidemic agent	PPAR-α agonist
Nafenopin	Hypolipidemic agent	PPAR-α agonist
Rosiglitazone	Antidiabetic agent	PPAR-γ agonist
Valproic Acid	Antiepileptic	Voltage-gated Na^+ channel blocker

TABLE 3
Biological pathways significantly impacted by A-875400 (R), A-908292 (S), and bezafibrate in rat liver

Pathway	Compound	No. of Regulated Genes in Pathway	Total No. of Genes in Pathway	Intersection	p Value
				%	
PPAR-α and fatty acid metabolism	A-875400 (R)	11	47	23.4	7.0E-6
	A-908292 (S)	12	47	25.5	1.0E-7
	Bezafibrate	16	47	34.0	6.2E-12
Bile acid and cholesterol metabolism	A-875400 (R)	11	54	20.4	2.9E-5
	A-908292 (S)	14	54	25.9	7.3E-9
	Bezafibrate	15	54	27.8	7.5E-10
Regulation of fatty acid biosynthesis	A-875400 (R)	10	58	17.2	2.8E-4
	A-908292 (S)	11	58	19.0	8.4E-6
	Bezafibrate	12	58	20.7	1.3E-6
Fatty acid biosynthesis	A-875400 (R)	4	16	25.0	5.2E-3
	A-908292 (S)	6	16	37.5	1.5E-5
	Bezafibrate	6	16	37.5	1.5E-5
β-Oxidation of fatty acid	A-875400 (R)	3	22	13.6	4.7E-2
	A-908292 (S)	4	22	18.2	8.3E-3
	Bezafibrate	3	22	13.6	4.7E-2

A-875400 (R) and A-908292 (S). Bezafibrate was included as a positive control. Electron microscopy analysis confirmed that all three compounds resulted in an increased number of peroxisomes relative to vehicle-treated control. The results for bezafibrate and A-875400 (R) are shown in Fig. 6C.

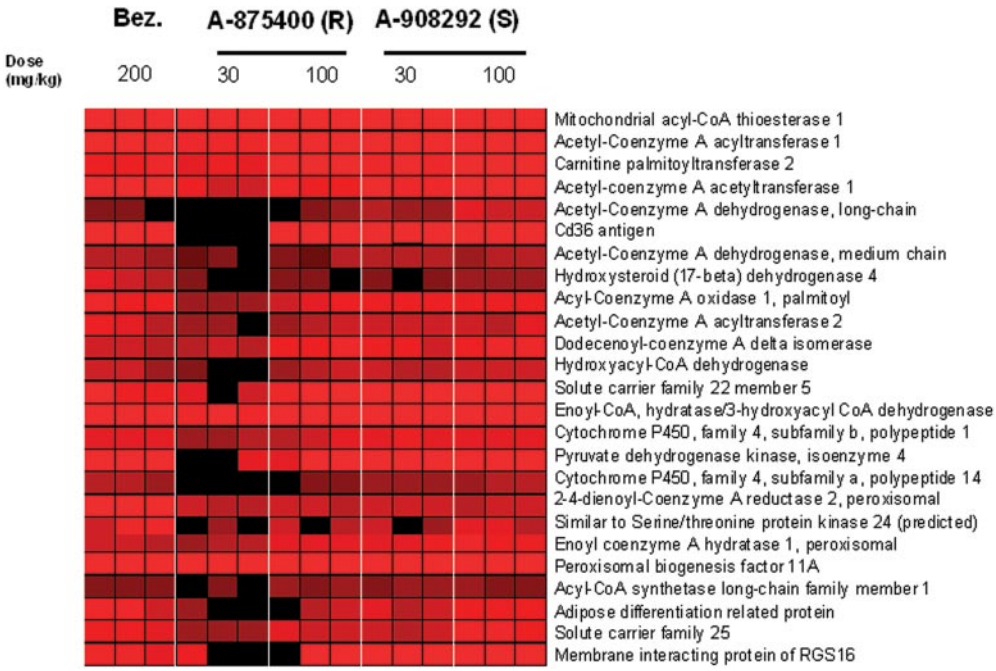

Fig. 5. Comparison of liver expression profiles for genes in the PPAR-α pathway from rats (n = 3/treatment group) treated for 3 days with the reference PPAR-α agonist bezafibrate at 200 mg/kg or A-875400 (R) and A-908292 (S) at 30 and 100 mg/kg. The gene expression analysis from bezafibrate-treated rats is from historical data run in our laboratory.

TABLE 4

Log(10) ratio values from isolated rat hepatocytes treated with A-875400 (R) or A-908292 (S) for the 11 genes in the in vitro PPAR-α signature, as well as other genes involved in PPAR-α activation

Values shown are biological replicates.

A-875400 (R)		A-908292 (S)		Sequence Description
1	2	1	2	
−0.04	0.10	0.04	0.01	Cytochrome P450, family 2, subfamily d, polypeptide 13
−0.35	−0.14	0.03	−0.29	Formiminotransferase cyclodeaminase
0.24	0.16	0.16	0.16	Sterol regulatory element binding factor 1
0.58	0.52	0.57	0.57	Mitochondrial acyl-CoA thioesterase 1
0.16	0.16	0.14	0.16	Acetyl-CoA acyltransferase 1
0.53	0.51	0.45	0.48	Cytosolic acyl-CoA thioesterase 1
0.41	0.36	0.53	0.53	Acyl-CoA synthetase long-chain family member 1
0.26	0.17	0.45	0.31	Acyl-CoA thioesterase 7
−0.11	−0.08	−0.15	−0.10	All-trans-13,14-dihydroretinol saturase
−0.04	−0.13	−0.19	−0.15	Epoxide hydrolase 2, cytoplasmic
0.02	−0.08	−0.17	−0.04	Estrogen sulfotransferase
0.41	0.36	0.53	0.53	Acyl-CoA synthetase long-chain family member 1
0.24	0.18	0.20	0.14	Acyl-CoA dehydrogenase, short/branched chain
0.16	0.15	0.20	0.21	Acyl-CoA oxidase 1, palmitoyl

Cross-Species Analysis. It was of interest to determine whether the effects on PPAR-α seen in rodents by A-908292 (S) and A-875400 (R) would also occur in humans. To determine this, the compounds were evaluated for their ability to directly activate human PPAR-α using a luciferase reporter assay containing the human PPAR-α ligand binding domain fused to the Gal4 DNA binding domain. Although the known PPAR-α ligand, GW7647 robustly activated the PPAR-α reporter, neither A-875400 (R) nor A-908292 (S) significantly activated PPAR-α (Fig. 7). To further assess the effects of these compounds in a human cell system, isolated human hepatocytes were treated with A-875400 (R) or A-908292 (S) at concentrations of 50 or 100 μM, and quantitative polymerase chain reaction was performed for two downstream genes of PPAR-α, cytochrome P450 4A11 and HMGCS2 (Marcus et al., 1993). Both of these genes were induced to some degree by the positive controls fenofibric acid, clofibric acid, and pirinixic acid; however, no induction was seen with either A-908292 (S) or A-875400 (R) (Fig. 8). The results suggest that the activation of the PPAR-α pathway with A-908292 (S) and A-875400 (R) may be rodent-specific.

Discussion

Based largely on the ACC2 knock-out mouse phenotype, we envision that small-molecule inhibitors against ACC2 would be efficacious for targeting obesity, dyslipidemia, and metabolic diseases. In a previous test, we established malonyl-CoA as the key biomarker for on-target ACC inhibition; from this, we identified a potent ACC2 inhibitor, compound A-859610, a racemic mixture of A-908292 (S) and A-875400 (R). Further studies showed that only the (S)enantiomer of A-859610, A-908292 (S), was able to reduce skeletal muscle malonyl-CoA, but not the (R)enantiomer. However, the conundrum was that both enantiomers lowered glucose and triglycerides in *ob/ob* mice. In this study, we present gene expression data that supports the hypothesis that both enantiomers modulate the PPAR-α signaling pathway.

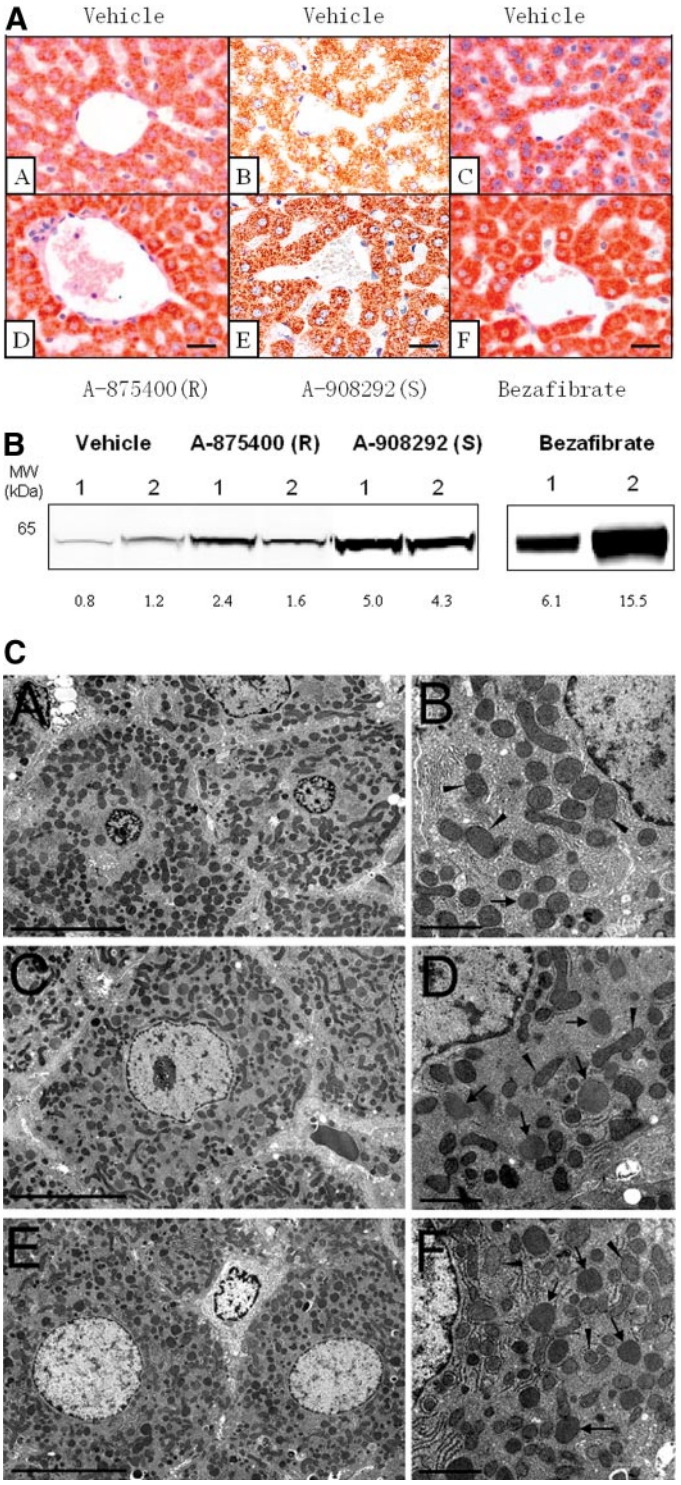

Fig. 6. A, immunohistochemistry staining for PMP70 in liver for rats treated for 3 or 5 days with vehicle, bezafibrate (200 mg/kg), A-908292 (S) (100 mg/kg), or A-875400 (R) (100 mg/kg). Magnification bars, 25 μm. B, Western blot showing protein levels of PMP70 in livers from rats treated with vehicle, A-875400 (R), A-908292 (S), or bezafibrate. The numbers below the band indicate PMP70 levels relative to the average of vehicle-treated controls. C, electron microscopy of livers from rats treated with A-875400 (R), bezafibrate, or vehicle. Magnification bars on plates A, C, and E, 10 μm. Bars on plates B, D, and F, 2 μm. Arrowheads, mitochondria; full arrows, peroxisomes. A and B, vehicle-treated control (Tween Vehicle); C and D, A-875400 (R) (100 mg/kg); E and F, bezafibrate (200 mg/kg).

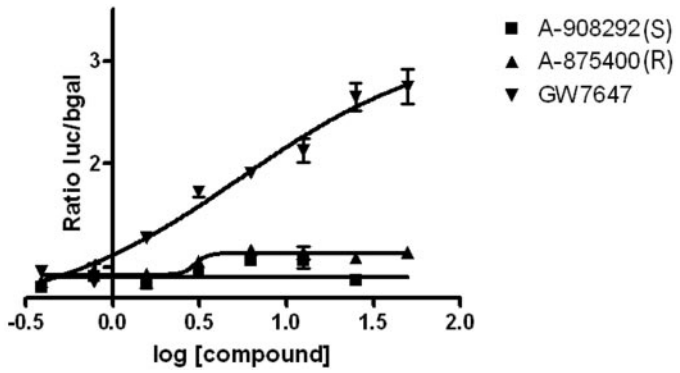

Fig. 7. Activation of a human PPAR-α luciferase reporter construct with GW7647, A-875400 (R), or A-908292 (S) in HepG2 cells. HepG2 cells were treated at concentrations ranging from 0.003 to 30 μM for A-875400 (R) or A-908292 (S). Cells were treated at concentrations ranging from 0.003 to 30 nM for GW7647. The x-axis shows log10 levels of the treatment compound. Concentrations of GW7647 are in nanomolar, whereas A-908292 (S) and A-875400 (R) are in micromolar. The y-axis shows luciferase units standardized relative to the internal control, pCMVbgal.

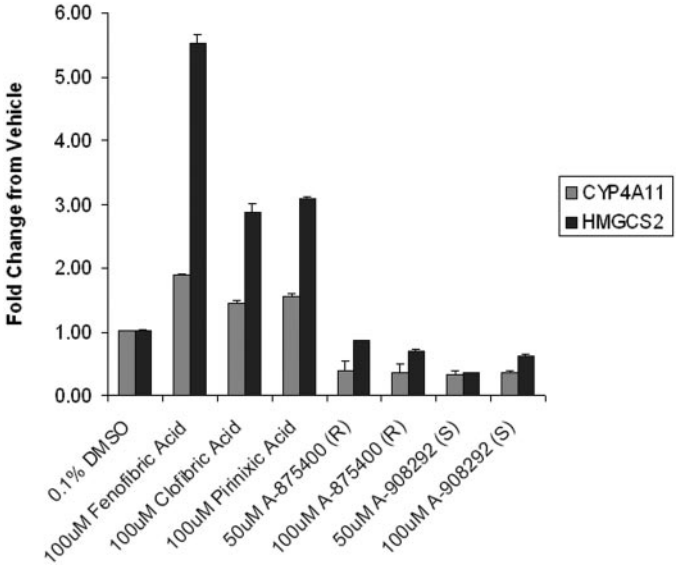

Fig. 8. Real-time polymerase chain reaction analysis for the induction of two downstream genes of PPAR-α, cytochrome P450 4A11 (CYP4A11) and HMGCS2 in isolated human hepatocytes treated with vehicle, or the PPAR-α agonists fenofibric acid, clofibrate, and pirinix acid compared with A-875400 (R) or A-908292 (S). The graph shows the -fold change of the two genes resulting from compound treatment relative to vehicle treated controls. The results shown are the average from an n of 2 for each treatment group. Error bars, S.D.

PPAR-α is a ligand-activated transcription factor belonging to the nuclear receptor superfamily and is known to be activated by numerous compounds, such as the fibrate class of drugs used to treat hyperlipidemia or several industrials plasticizers (Grundy and Vega, 1987). Compounds known to activate PPAR-α are also referred to as peroxisome proliferators because they cause peroxisome proliferation in rodents. Histopathologic evaluation further supported the finding that A-908292 (S) and A-875400 (R) induced peroxisome proliferation in the rats. Livers from rats treated for 3 days with A-908292 (S) and A-875400 (R) showed increased mitotic activity and minimal hepatocellular hypertrophy, histological findings previously reported in studies with rats treated with known PPAR-α activators (Baker et al., 2004). Results from Western blot and immunohistochemical staining dem-

onstrated that both A-908292 (S) and A-875400 (R) caused an increase in the levels of PMP70, a marker for peroxisome proliferation. Finally, electron microscopy, which allows for a definitive determination of peroxisome proliferation, confirmed that both A-908292 (S) and A-875400 (R) induced peroxisome proliferation in treated rat liver (Cattley, 2002).

The possibility that A-908292 (S) and A-875400 (R) may be activators of the PPAR-α pathway are consistent with the pharmacology results in *ob*/*ob* mice, which showed glucose and triglyceride lowering observed with both the active and inactive enantiomers. Previous results have shown that PPAR-α activators can improve glucose homeostasis and lower plasma triglyceride levels in mouse models for type II diabetes (Kim et al., 2003). Based on the present data, most likely the glucose and triglyceride lowering by the compounds are primarily mediated by PPAR-α activation. However, it was interesting to note that there was no further lowering of glucose or triglyceride by the active A-908292 (S) compared with A-875400 (R). It is possible that ACC inhibition and PPAR-α activation both converge onto a same metabolic pathway.

The activation of the PPAR-α pathway by A-908292 (S) and A-875400 (R) could be a result of direct binding and activation of PPAR-α by the compounds, or it could be through secondary mechanisms. Secondary mechanisms for activation of PPAR-α have been previously proposed. For instance, Kaikaus et al. (1993) hypothesized that some peroxisome proliferators act by inhibiting carnitine palmitoyltransferase I, resulting in increased levels of long-chain dicarboxylic acids, which serve as the inducers of PPAR-α. Other research has shown that changes in phosphorylation can result in PPAR-α activation or repression (Burns and Vanden Heuvel, 2007). Whether A-908292 (S) and A-875400 (R) are direct or indirect activators of the PPAR-α pathway is unclear; however, the activation does not seem to be solely mediated by ACC2 inhibition because A-875400 (R) is a very weak ACC2 inhibitor.

Treatment with A-908292 (S) results in an increased number of liver gene expression changes relative to A-875400 (R). This could be due to the lower drug levels in the liver for A-875400 (R) (Fig. 4). However, some of these gene expression changes may be related to inhibition of ACC2. We performed ANOVA to identify gene expression changes unique to A-908292 (S) relative to A-875400 (R). Approximately 75 genes were identified that were significantly differentially regulated between the two compounds (data not shown). Many of these genes were expressed sequence tags or belong to the PPAR-α pathway, such as acetyl-CoA acetyltransferase 1 and acetyl-CoA synthetase long-chain family member 3. Thus, a clear gene expression signature that might correlate with ACC2 inhibition could not be identified.

Analysis of the compounds in vitro showed that both compounds activated the PPAR-α pathway in isolated rat hepatocytes but did not have the same effect in isolated human hepatocytes or in a human PPAR-α reporter system. The results suggest that interaction with the PPAR-α pathway by these compounds may be species-specific. These results are in keeping with previous studies, which have shown marked species differences in response to peroxisome proliferators (Cattley et al., 1998; Vanden Heuvel, 1999). Studies to understand the underlying cause for the PPAR-α species specificity have identified differences in the promoter regions of human and rodent PPAR-α target genes and suggest that additional coregulators of PPAR-α in rodent and human hepatocytes may contribute as well (Ammerschlaeger et al., 2004).

In summary, we have used gene expression analysis to identify a possible mechanism to explain the glucose- and triglyceride-lowering effects of active and inactive ACC2 inhibitors. Other studies have shown that gene expression analysis can be an extremely useful tool for discerning the pharmacological or toxicological mechanisms of xenobiotic agents (Waring et al., 2002; Wang, 2005; Maloney et al., 2007). By using gene expression analysis, we were able to conclude that the metabolic activity of A-908292 (S) and A-875400 (R) were probably mediated, at least partly, through PPAR-α and not solely by ACC2 inhibition. Further studies using inhibitors of ACC2 without the PPAR-α activity will help to elucidate the role of this target in metabolic disease syndromes.

Acknowledgments

We thank Michael Liguori, Amy Ditewig, Gerard Gagne, Margery Stark, and Jane Fagerland for technical assistance.

References

Abu-Elheiga L, Almarza-Ortega DB, Baldini A, and Wakil SJ (1997) Human acetyl-CoA carboxylase 2: molecular cloning, characterization, chromosomal mapping, and evidence for two isoforms. *J Biol Chem* **272:**10669–10677.

Abu-Elheiga L, Brinkley WR, Zhong L, Chirala SS, Woldegiorgis G, and Wakil SJ (2000) The subcellular localization of acetyl-CoA carboxylase 2. *Proc Natl Acad Sci U S A* **97:**1444–1449.

Abu-Elheiga L, Matzuk MM, Abo-Hashema KA, and Wakil SJ (2001) Continuous fatty acid oxidation and reduced fat storage in mice lacking acetyl-CoA carboxylase 2. *Science* **291:**2613–2616.

Ammerschlaeger M, Beigel J, Klein KU, and Mueller SO (2004) Characterization of the species-specificity of peroxisome proliferators in rat and human hepatocytes. *Toxicol Sci* **78:**229–240.

Baker VA, Harries HM, Waring JF, Duggan CM, Ni HA, Jolly RA, Yoon LW, De Souza AT, Schmid JE, Brown RH, et al. (2004) Clofibrate-induced gene expression changes in rat liver: a cross-laboratory analysis using membrane cDNA arrays. *Environ Health Perspect* **112:**428–438.

Burns KA and Vanden Heuvel JP (2007) Modulation of PPAR activ0ity via phosphorylation. *Biochim Biophys Acta* **1771:**952–960.

Cattley RC (2002) *Handbook of Toxicologic Pathology*, Academic Press, New York.

Cattley RC, DeLuca J, Elcombe C, Fenner-Crisp P, Lake BG, Marsman DS, Pastoor TA, Popp JA, Robinson DE, Schwetz B, et al. (1998) Do peroxisome proliferating compounds pose a hepatocarcinogenic hazard to humans? *Regul Toxicol Pharmacol* **27:**47–60.

Colton HM, Falls JG, Ni H, Kwanyuen P, Creech D, McNeil E, Casey WM, Hamilton G, and Cariello NF (2004) Visualization and quantitation of peroxisomes using fluorescent nanocrystals: treatment of rats and monkeys with fibrates and detection in the liver. *Toxicol Sci* **80:**183–192.

Ganter B, Tugendreich S, Pearson CI, Ayanoglu E, Baumhueter S, Bostian KA, Brady L, Browne LJ, Calvin JT, Day GJ, et al. (2005) Development of a large-scale chemogenomics database to improve drug candidate selection and to understand mechanisms of chemical toxicity and action. *J Biotechnol* **119:**219–244.

Gao L, Chiou W, Tang H, Cheng X, Camp HS, and Burns DJ (2007) Simultaneous quantification of malonyl-CoA and several other short-chain acyl-CoAs in animal tissues by ion-pairing reversed-phase HPLC/MS. *J Chromatogr B Analyt Technol Biomed Life Sci* **853:**303–313.

Grundy SM and Vega GL (1987) Fibric acids: effects on lipids and lipoprotein metabolism. *Am J Med* **83:**9–20.

Gu YG, Weitzberg M, Clark RF, Xu X, Li Q, Zhang T, Hansen TM, Liu G, Xin Z, Wang X, et al. (2006) Synthesis and structure-activity relationships of *N*-{3-[2-(4-alkoxyphenoxy)thiazol-5-yl]-1-methylprop-2-ynyl}carboxy derivatives as selective acetyl-CoA carboxylase 2 inhibitors. *J Med Chem* **49:**3770–3773.

Hsu HL, Wadman I, and Baer R (1994) Formation of in vivo complexes between the TAL1 and E2A polypeptides of leukemic T cells. *Proc Natl Acad Sci U S A* **91:**3181–3185.

Hulver MW, Berggren JR, Cortright RN, Dudek RW, Thompson RP, Pories WJ, MacDonald KG, Cline GW, Shulman GI, Dohm GL, et al. (2003) Skeletal muscle lipid metabolism with obesity. *Am J Physiol Endocrinol Metab* **284:**E741–E747.

Kaikaus RM, Chan WK, Lysenko N, Ray R, Ortiz de Montellano PR, and Bass NM (1993) Induction of peroxisomal fatty acid beta-oxidation and liver fatty acid-binding protein by peroxisome proliferators: mediation via the cytochrome P-450IVA1 omega-hydroxylase pathway. *J Biol Chem* **268:**9593–9603.

Kim H, Haluzik M, Asghar Z, Yau D, Joseph JW, Fernandez AM, Reitman ML, Yakar S, Stannard B, Heron-Milhavet L, et al. (2003) Peroxisome proliferator-activated receptor-α agonist treatment in a transgenic model of type 2 diabetes reverses the lipotoxic state and improves glucose homeostasis. *Diabetes* **52:**1770–1778.

Lehmann JM, Moore LB, Smith-Oliver TA, Wilkison WO, Willson TM, and Kliewer SA (1995) An antidiabetic thiazolidinedione is a high affinity ligand for peroxisome proliferator-activated receptor γ (PPARγ). *J Biol Chem* **270:**12953–12956.

Maloney A, Clarke PA, Naaby-Hansen S, Stein R, Koopman JO, Akpan A, Yang A, Zvelebil M, Cramer R, Stimson L, et al. (2007) Gene and protein expression profiling of human ovarian cancer cells treated with the heat shock protein 90 inhibitor 17-allylamino-17-demethoxygeldanamycin. *Cancer Res* **67:**3239–3253.

Mao J, Chirala SS, and Wakil SJ (2003) Human acetyl-CoA carboxylase 1 gene: presence of three promoters and heterogeneity at the 5′-untranslated mRNA region. *Proc Natl Acad Sci U S A* **100:**7515–7520.

Marcus SL, Miyata KS, Zhang B, Subramani S, Rachubinski RA, and Capone JP (1993) Diverse peroxisome proliferator-activated receptors bind to the peroxisome proliferator-responsive elements of the rat hydratase/dehydrogenase and fatty acyl-CoA oxidase genes but differentially induce expression. *Proc Natl Acad Sci U S A* **90:**5723–5727.

Oh W, Abu-Elheiga L, Kordari P, Gu Z, Shaikenov T, Chirala SS, and Wakil SJ (2005) Glucose and fat metabolism in adipose tissue of acetyl-CoA carboxylase 2 knockout mice. *Proc Natl Acad Sci U S A* **102:**1384–1389.

Ruderman N and Prentki M (2004) AMP kinase and malonyl-CoA: targets for therapy of the metabolic syndrome. *Nat Rev Drug Discov* **3:**340–351.

Sinha R, Dufour S, Petersen KF, LeBon V, Enoksson S, Ma YZ, Savoye M, Rothman DL, Shulman GI, and Caprio S (2002) Assessment of skeletal muscle triglyceride content by ^{1}H nuclear magnetic resonance spectroscopy in lean and obese adolescents: relationships to insulin sensitivity, total body fat, and central adiposity. *Diabetes* **51:**1022–1027.

Steyn NP, Mann J, Bennett PH, Temple N, Zimmet P, Tuomilehto J, Lindstrom J, and Louheranta A (2004) Diet, nutrition and the prevention of type 2 diabetes. *Public Health Nutr* **7:**147–165.

Turkoglu C, Duman BS, Gunay D, Cagatay P, Ozcan R, and Buyukdevrim AS (2003) Effect of abdominal obesity on insulin resistance and the components of the metabolic syndrome: evidence supporting obesity as the central feature. *Obes Surg* **13:**699–705.

Vanden Heuvel JP (1999) Peroxisome proliferator-activated receptors (PPARS) and carcinogenesis. *Toxicol Sci* **47:**1–8.

Wang Y (2005) Gene expression-driven diagnostics and pharmacogenomics in cancer. *Curr Opin Mol Ther* **7:**246–250.

Waring JF, Ciurlionis R, Clampit JE, Morgan S, Gum RJ, Jolly RA, Kroeger P, Frost L, Trevillyan J, Zinker BA, et al. (2003) PTP1B antisense-treated mice show regulation of genes involved in lipogenesis in liver and fat. *Mol Cell Endocrinol* **203:**155–168.

Waring JF, Ciurlionis R, Jolly RA, Heindel M, and Ulrich RG (2001a) Microarray analysis of hepatotoxins in vitro reveals a correlation between gene expression profiles and mechanisms of toxicity. *Toxicol Lett* **120:**359–368.

Waring JF, Gum R, Morfitt D, Jolly RA, Ciurlionis R, Heindel M, Gallenberg L, Buratto B, and Ulrich RG (2002) Identifying toxic mechanisms using DNA microarrays: evidence that an experimental inhibitor of cell adhesion molecule expression signals through the aryl hydrocarbon nuclear receptor. *Toxicology* **181–182:**537–550.

Waring JF, Jolly RA, Ciurlionis R, Lum PY, Praestgaard JT, Morfitt DC, Buratto B, Roberts C, Schadt E, and Ulrich RG (2001b) Clustering of hepatotoxins based on mechanism of toxicity using gene expression profiles. *Toxicol Appl Pharmacol* **175:**28–42.

Xu X, Weitzberg M, Keyes RF, Li Q, Wang R, Wang X, Zhang X, Frevert EU, Camp HS, Beutel BA, et al. (2007) The synthesis and structure-activity relationship studies of selective acetyl-CoA carboxylase inhibitors containing 4-(thiazol-5-yl)but-3-yn-2-amino motif: polar region modifications. *Bioorg Med Chem Lett* **17:**1803–1807.

Yang Y, Abel SJ, Ciurlionis R, and Waring JF (2006) Development of a toxicogenomics in vitro assay for the efficient characterization of compounds. *Pharmacogenomics* **7:**177–186.

Zinker BA, Rondinone CM, Trevillyan JM, Gum RJ, Clampit JE, Waring JF, Xie N, Wilcox D, Jacobson P, Frost L, et al. (2002) PTP1B antisense oligonucleotide lowers PTP1B protein, normalizes blood glucose, and improves insulin sensitivity in diabetic mice. *Proc Natl Acad Sci U S A* **99:**11357–11362.

Address correspondence to: Dr. Jeffrey F. Waring, Molecular and Cellular Toxicology, Abbott Laboratories, Building AP9A R463, 100 Abbott Park Road, Abbott Park, IL 60064-6125. E-mail: jeff.waring@abbott.com